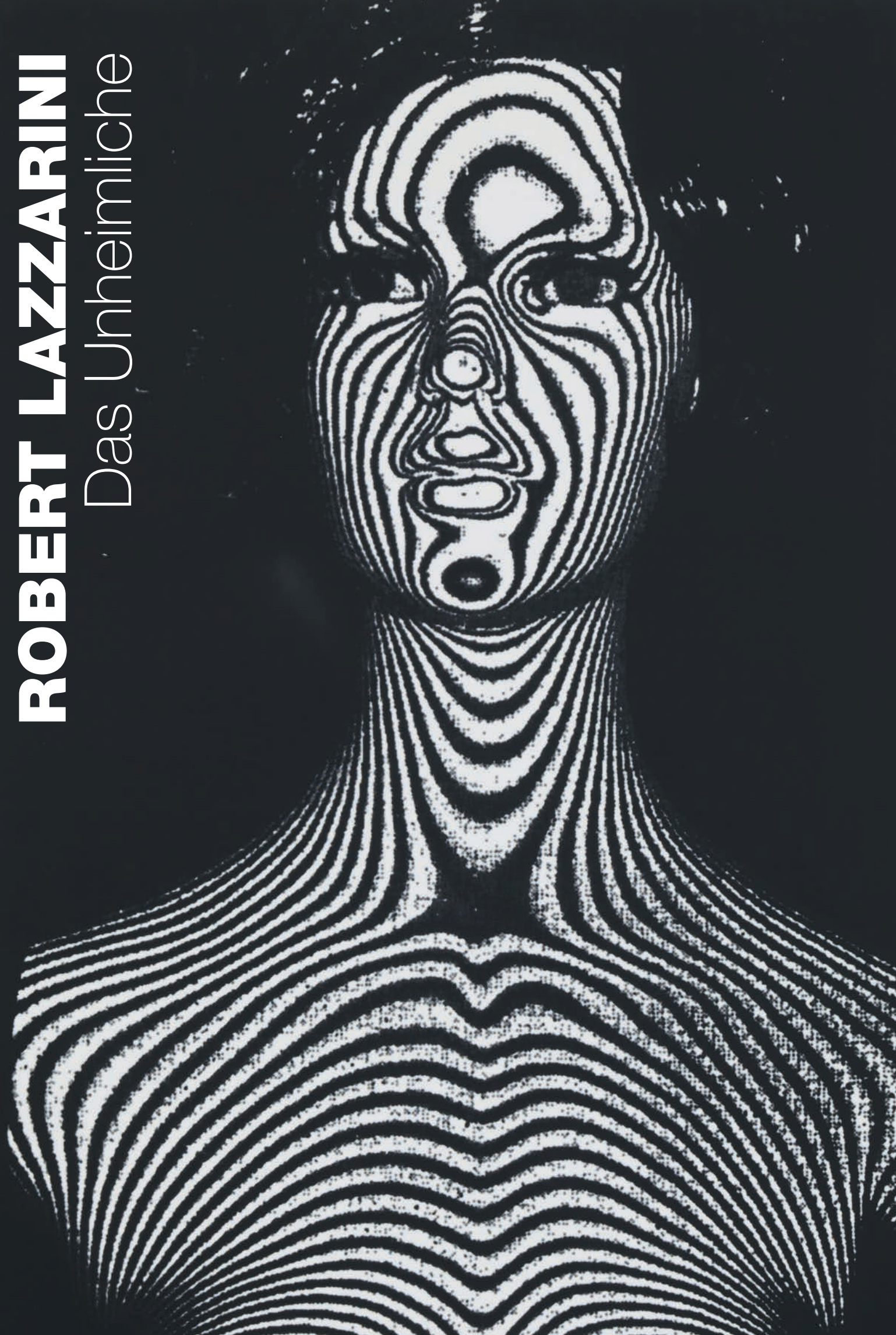


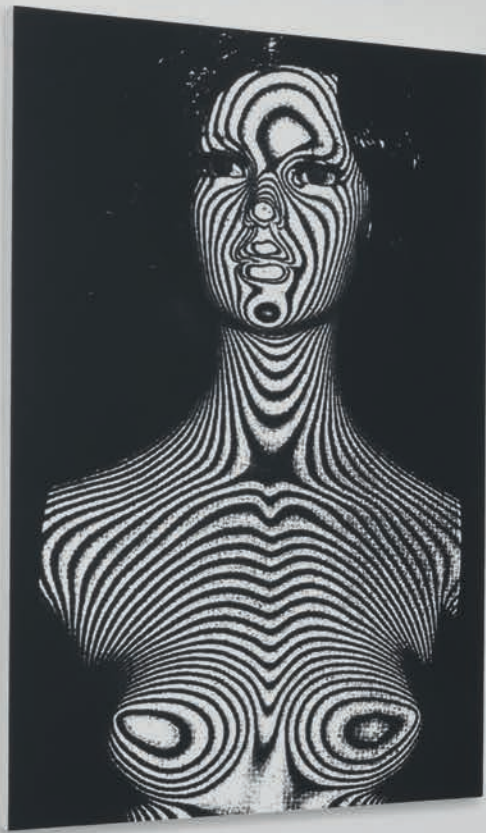
ROBERT LAZZARINI

Das Unheimliche



ROBERT LAZZARINI

Das Unheimliche





Previous page, left:
M2, 2014
acrylic on canvas
134.62 x 83.82 cm / 53 x 33 inches

Previous page, right:
M2, 2014
Detail view

Removal of Unwanted Patterns from Moiré Contour Maps by Grid Translation Techniques

J. B. Allen and D. M. Meadows

Lockheed-Georgia Company, Marietta, Georgia 30060.
Received 3 September 1970.

The generation of surface contours by moiré pattern techniques has been described recently.^{1,2} Both papers point out that one problem with moiré contouring techniques is the noncontour patterns produced along with the moiré patterns. The noncontour or unwanted patterns can obscure the true contours or degrade the quality of the contour map. Figure 1 is a contour map of a nose section of a C-5A Galaxy wind tunnel model. Note that the contours are so obscured by the unwanted patterns that they are, for all practical purposes, not visible. Takasaki² points out that by translating the grid in its plane, the unwanted patterns can be removed leaving only the contours. The limitations of the moving grid technique and a detailed analysis of how the technique works is presented in this Letter.

The means by which surface contours are generated by moiré patterns and the manner in which the above-mentioned unwanted lines arise was described in detail in Ref. 1. To generate surface contours by the moiré method, a light source, not necessarily coherent, illuminates a grid as shown in Fig. 2. If the grid is coarse enough and the surface to be contoured is close enough to the grid that the effects of diffraction can be ignored, the shadow of the grid is essentially projected onto the surface. When an observer or camera at the same height as the light source views the surface through the grid, the moiré interference of the grid with its shadow on the surface will be evident. This moiré interference produces the contour map of the surface as well as certain unwanted patterns. It is shown in Ref. 1 that, when the grid is

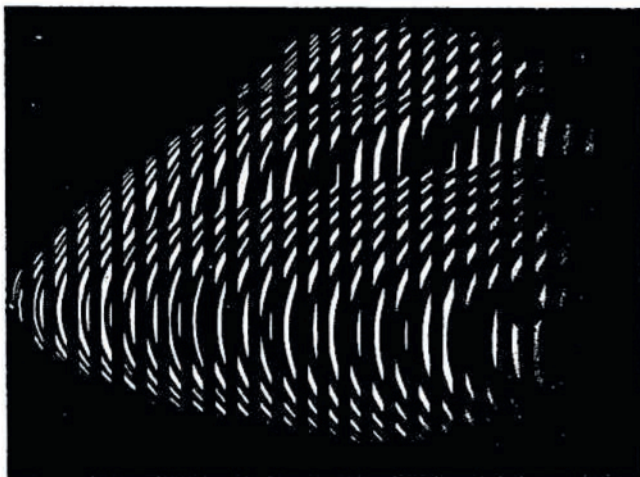


Fig. 1. Moiré contour map of a C-5A nose section with none of the unwanted patterns removed.

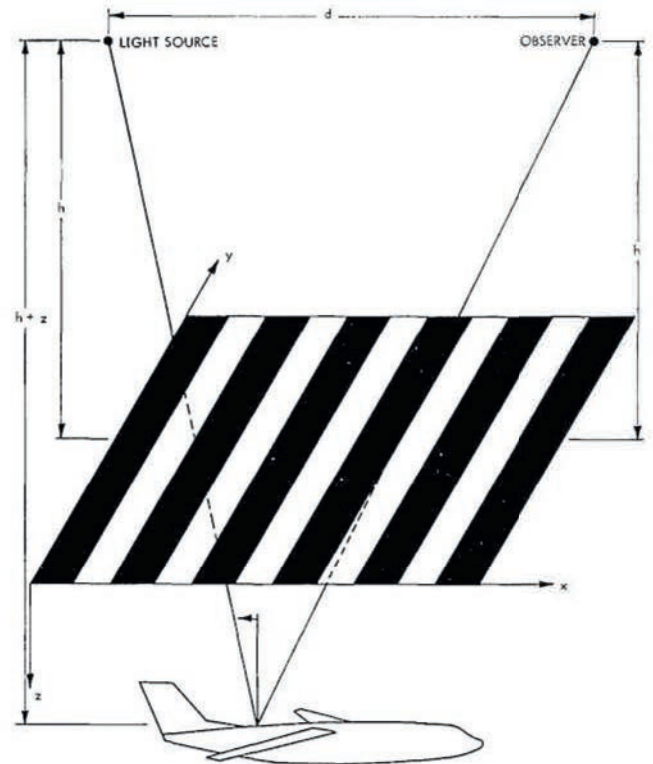


Fig. 2. Schematic of the arrangement used to make moiré contour maps.

sinusoidal of period p with an intensity transmission $T_1(x)$ given by

$$T_1(x) = \frac{1}{2} + \frac{1}{2} \sin \frac{2\pi x}{p}, \tag{1}$$

the intensity $I_1(x,y)$ pattern will be seen by the observer:

$$\begin{aligned} I_1(x,y) &= C \left[\frac{1}{2} + \frac{1}{2} \sin \frac{2\pi hx}{p(h+z)} \right] \left[\frac{1}{2} + \frac{1}{2} \sin \frac{2\pi}{p} \left(\frac{dz+hx}{h+z} \right) \right] \\ &= \frac{C}{4} \left[1 + \sin \frac{2\pi}{p} \left(\frac{hx}{h+z} \right) + \sin \frac{2\pi}{p} \left(\frac{dz+hx}{h+z} \right) \right. \\ &\quad \left. - \frac{1}{2} \cos \frac{2\pi}{p} \left(\frac{2hx+dz}{h+z} \right) + \frac{1}{2} \cos \frac{2\pi}{p} \left(\frac{dz}{h+z} \right) \right]. \tag{2} \end{aligned}$$

C is a constant, h is the height of the light and observer, and $z(x,y)$ is the depth of the surface below the grid at the point (x,y) . The last term in Eq. (2) is solely dependent on height and is the contour term. The other three sinusoidal terms, although height-dependent, are also dependent on x and, hence, do not represent contours. The patterns corresponding to these three terms can obscure the contours as shown in Fig. 1.

One means of removing the unwanted patterns is to make four exposures on the film with the grid in four different positions, each position separated by a distance of $p/4$. The resulting picture will have no unwanted terms or noncontour patterns. To be more precise, suppose that the film in the camera is exposed recording the intensity pattern as specified in Eq. (2). Now, let us translate the grid by a distance of $p/4$ so that the intensity transmission of the grid is given by:

$$T'_1(x) = \frac{1}{2} + \frac{1}{2} \cos(2\pi x/p). \tag{3}$$

Let us now expose the film with the grid in the position indicated by Eq. (3). The intensity $I_1(x,y)$ recorded by the film can be shown by an analysis similar to the one above, to be

$$I_1(x,y) = \frac{C}{4} \left[1 + \cos \frac{2\pi x h}{p(h+z)} + \cos \frac{2\pi}{p} \left(\frac{dz + hx}{h+z} \right) + \frac{1}{2} \cos \frac{2\pi}{p} \left(\frac{dz + hx}{h+z} \right) + \frac{1}{2} \cos \frac{2\pi}{p} \left(\frac{dz}{h+z} \right) \right]. \quad (4)$$

If the grid is then translated by distances $p/2$ and $3p/4$, the intensity transmission of the grid will, respectively, be

$$T''_1(x) = \frac{1}{2} - \frac{1}{2} \sin \frac{2\pi x}{p} \quad (5)$$

and

$$T'''_1(x) = \frac{1}{2} - \frac{1}{2} \cos \frac{2\pi x}{p}. \quad (6)$$

The resulting intensity patterns recorded by the camera will then be, respectively,

$$I''_1(x,y) = \frac{C}{4} \left[1 - \sin \frac{2\pi hx}{p(h+z)} - \sin \frac{2\pi}{p} \left(\frac{hx + dz}{h+z} \right) - \frac{1}{2} \cos \frac{2\pi}{p} \left(\frac{dz + 2hx}{h+z} \right) + \frac{1}{2} \cos \frac{2\pi}{p} \left(\frac{dz}{h+z} \right) \right] \quad (7)$$

and

$$I'''_1(x,y) = \frac{C}{4} \left[1 - \cos \frac{2\pi hx}{p(h+z)} - \cos \frac{2\pi}{p} \left(\frac{dz + hx}{h+z} \right) + \frac{1}{2} \cos \frac{2\pi}{p} \left(\frac{dz + 2hx}{h+z} \right) + \frac{1}{2} \cos \frac{2\pi}{p} \left(\frac{dz}{h+z} \right) \right]. \quad (8)$$

If four equal duration exposures are made with the intensities $I_1(x,y)$, $I'_1(x,y)$, $I''_1(x,y)$, and $I'''_1(x,y)$, respectively, the resultant exposure of the film will be proportional to:

$$I = I_1(x,y) + I'_1(x,y) + I''_1(x,y) + I'''_1(x,y) = C \left[1 + \frac{1}{2} \cos \frac{2\pi}{p} \left(\frac{dz}{h+z} \right) \right]. \quad (9)$$

Note that the resulting exposure contains only the bias and contour terms.

By moving the grid to four successive positions during the exposure, we have managed to vary the unwanted terms so that they were canceled out, leaving only the contour term. The contour term was not canceled, because it is independent on the position of the grid. The advantage of this scheme compared to spatial filtering is that no contours are removed in translating the grid, regardless of their spatial frequency. Although this method is simple and workable, it can be improved. In its present form, it applies only to sinusoidal grids and requires precise translational positioning. This method will now be modified so that it will remove the unwanted terms created by a periodic grid, whether it is sinusoidal or not. The requirement to translate the grid precisely to four positions also will be removed.

It has been demonstrated in Ref. 1 that surface contours are produced with any periodic, one-dimensional grid. The particular shape of the contours is dependent on the shape of the grid, but the spacing of the contours is dependent only on the period of the grid. Specifically, let the grid have an arbitrarily shaped transmission function of period p specified by

$$T_2(x) = \frac{1}{2} + \frac{1}{2} g \left(\frac{2\pi x}{p} \right), \quad (10)$$

where $g(2\pi x/p)$ is a periodic function of period p and less or equal to 1 in absolute value. Expanding $g(2\pi x/p)$ in a Fourier series, we obtain:

$$T_2(x) = \frac{1}{2} + \frac{1}{2} \sum_1^{\infty} a_n \sin \frac{2\pi n x}{p} + b_n \cos \frac{2\pi n x}{p}, \quad (11)$$

where a_n and b_n are Fourier coefficients.

It is shown in Ref. 1 that the resulting intensity pattern seen by the observer is:

$$I_2(x,y) = C \left[\sum_1^{\infty} a_n \sin \left(\frac{2\pi n h x}{p(h+z)} \right) + b_n \cos \left(\frac{2\pi n h x}{p(h+z)} \right) + a_n \sin \left(\frac{2\pi n (dz + hx)}{p(h+z)} \right) + b_n \cos \left(\frac{2\pi n (dz + hx)}{p(h+z)} \right) + a_n b_n \sin \frac{2\pi n}{p} \left(\frac{dz + 2hx}{h+z} \right) + \frac{b_n^2 - a_n^2}{2} \cos \frac{2\pi n}{p} \left(\frac{dz + 2hx}{h+z} \right) + \sum_1^{\infty} \sum_{m \neq n} \left(\frac{a_m a_n + b_m b_n}{2} \right) \cos \frac{2\pi}{p} \left(\frac{(m-n)hx - ndz}{h+z} \right) + \left(\frac{b_m b_n - a_m a_n}{2} \right) \cos \frac{2\pi}{p} \left(\frac{(m+n)hx + ndz}{h+z} \right) + a_m b_n \sin \frac{2\pi}{p} \left(\frac{(m+n)hx + ndz}{h+z} \right) + 1 + \sum_1^{\infty} \left(\frac{a_n^2 + b_n^2}{2} \right) \cos \frac{2\pi n dz}{p(h+z)} \right]. \quad (12)$$

The last set of terms in Eq. (12), namely,

$$f(z) = C \left[1 + \sum_1^{\infty} \frac{1}{2} (a_n^2 + b_n^2) \cos \frac{2\pi}{p} \left(\frac{ndz}{h+z} \right) \right] \quad (13)$$

is the contour term, since it is independent of x and dependent only on z . As pointed out in Ref. 1, the period of the contours is dependent only on the period of the grid and not on its shape.

In Eq. (12), there are many noise terms which must be removed to make the contours plainly visible. Figure 1 illustrates the pattern indicated by Eq. (12). Since Eq. (12) contains terms of arbitrarily high frequencies, moving the grid to four different positions will not cancel all the noise terms. To cancel them all, one would have to move the grid to an infinite number of discrete positions. One way to accomplish this is to move the grid continuously during the exposure. To analyze what would happen if the grid is moving in time, the transmission function of the grid must also be made a function of time. If the grid is moving at a velocity v , the transmission function of the grid is given by:

$$T_2(x,t) = \frac{1}{2} + \frac{1}{2} g \left[\frac{2\pi}{p} (x - vt) \right] = \frac{1}{2} + \frac{1}{2} \sum_1^{\infty} a_n \sin \frac{2\pi n}{p} (x - vt) + b_n \cos \frac{2\pi n}{p} (x - vt). \quad (14)$$

Expanding Eq. (14) and regrouping terms, we obtain

$$T_2(x,t) = \frac{1}{2} + \frac{1}{2} \sum_1^{\infty} a'_n \sin \frac{2\pi n x}{p} + b'_n \cos \frac{2\pi n x}{p} \quad (15)$$

where

$$a'_n = a_n \cos \frac{2\pi n vt}{p} + b_n \sin \frac{2\pi n vt}{p} \quad \text{and} \quad b'_n = -a_n \sin \frac{2\pi n vt}{p} + b_n \cos \frac{2\pi n vt}{p}.$$

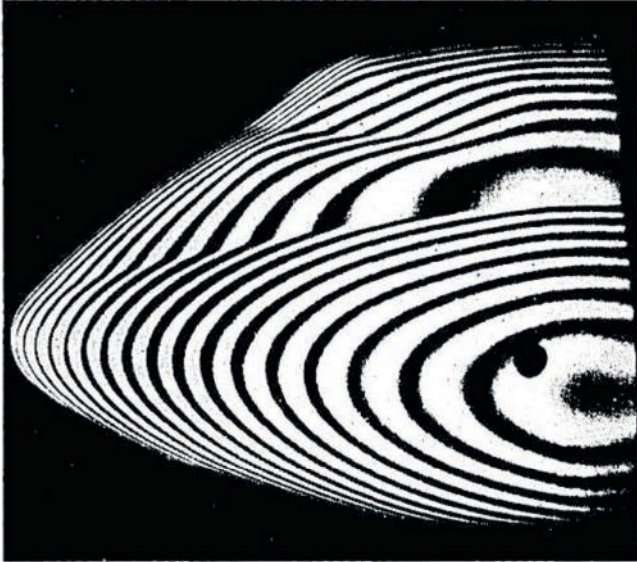


Fig. 3. Moiré contour map of the C-5A nose section with the unwanted patterns removed.

Equation (15) is identical to Eq. (11), except that the Fourier coefficients of Eq. (15) are functions of time. Hence all the Fourier coefficients of Eq. (15) are functions of time when the moving grid is used. Therefore, all the noise terms will be averaged out since the average of a sine wave over a period is zero. The expression for the contour term in the case of the moving grid is given by:

$$f(z) = C \left[1 + \sum_1^{\infty} \frac{1}{2} (a'^2_n + b'^2_n) \cos \frac{2\pi}{p} \left(\frac{ndz}{h+z} \right) \right]. \quad (16)$$

Substituting the expressions for a'_n and b'_n respectively, the above equation reduces to:

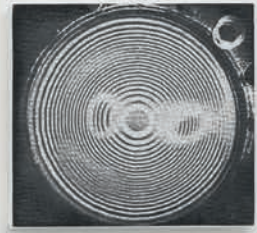
$$f(z) = C \left[1 + \sum_1^{\infty} \frac{1}{2} (a_n^2 + b_n^2) \cos \frac{2\pi}{p} \left(\frac{ndz}{h+z} \right) \right]. \quad (17)$$

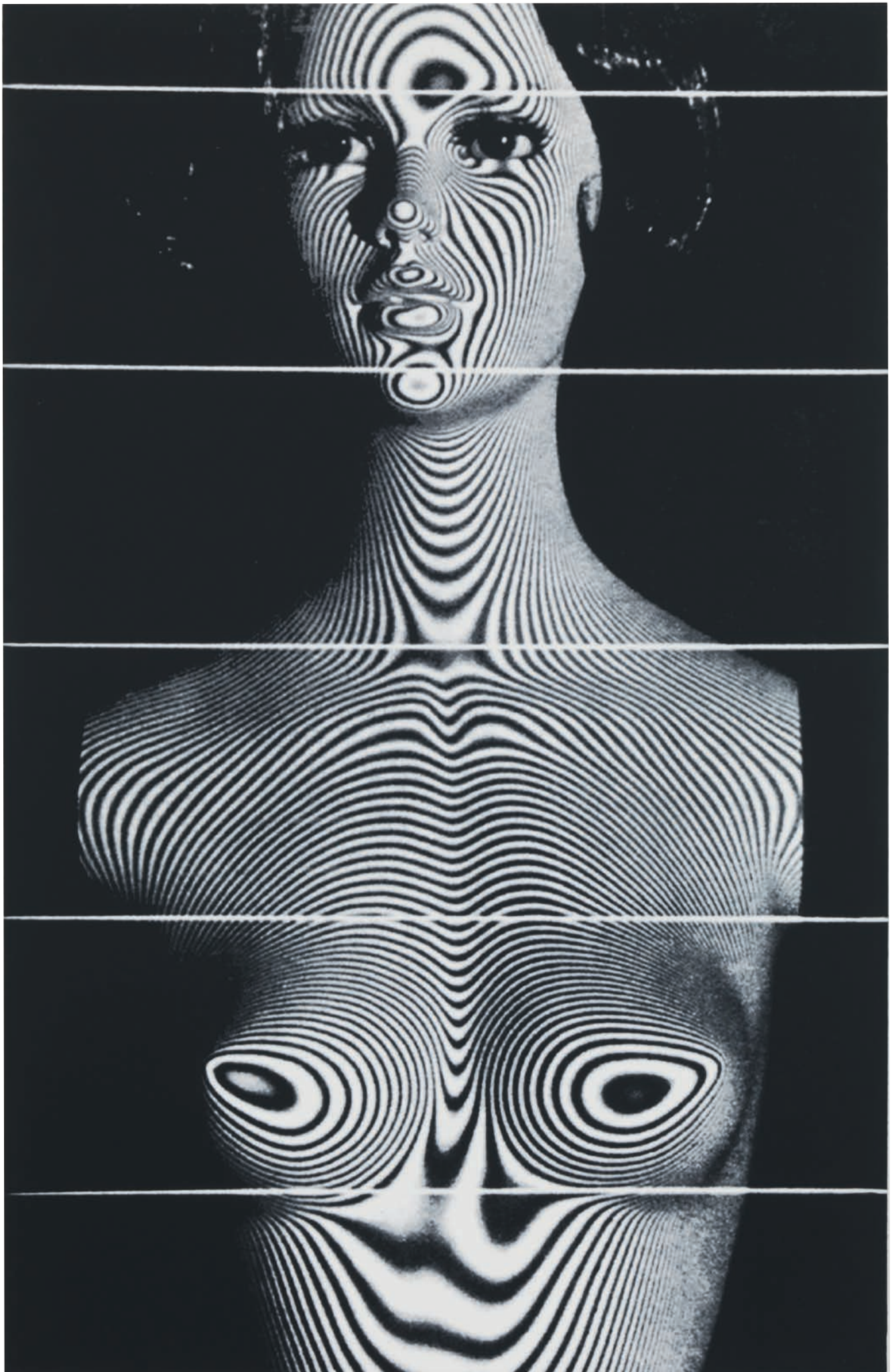
Hence, the time variation cancels out in the contour term and it is unaffected by the motion of the grid.

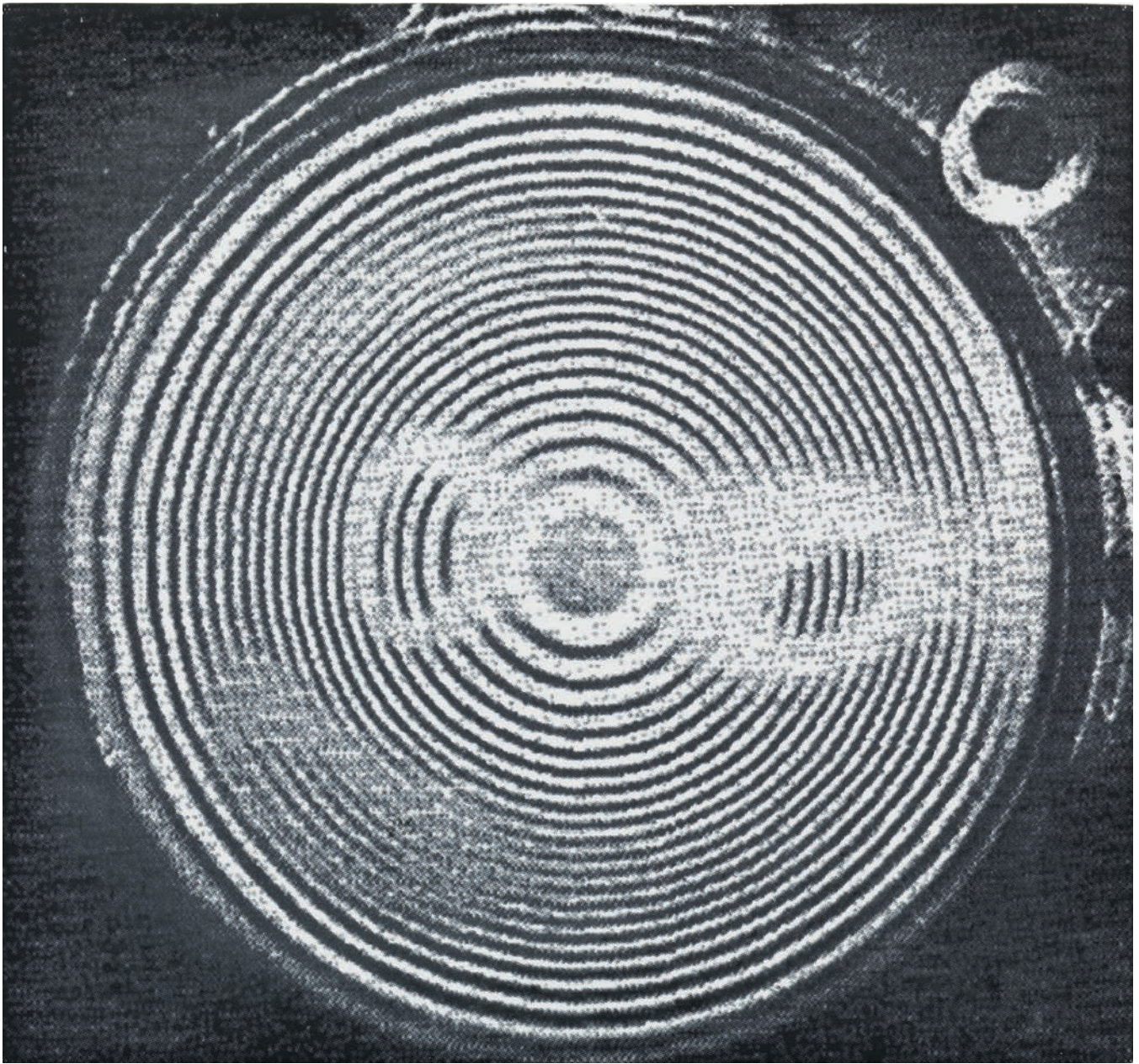
The continuously moving grid method is easier to implement than the discrete-translation method, since it does not require precise positioning of the grid at four positions. However, the motion of the grid must be uniform for all the unwanted terms to be canceled. The continuously moving grid method is more general because it removes the unwanted terms for any one-dimensional, periodic grid. Therefore, it is applicable to the most commonly used grid, namely, the square-wave grid. Figure 3 illustrates the effect of continuously moving the grid during the exposure. Note how the contours are much easier to see when the unwanted patterns have been removed.

References

1. D. M. Meadows, W. O. Johnson, and J. B. Allen, *Appl. Opt.* **9**, 942 (1970).
2. H. Takasaki, *Appl. Opt.* **9**, 1457 (1970).

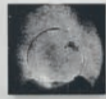


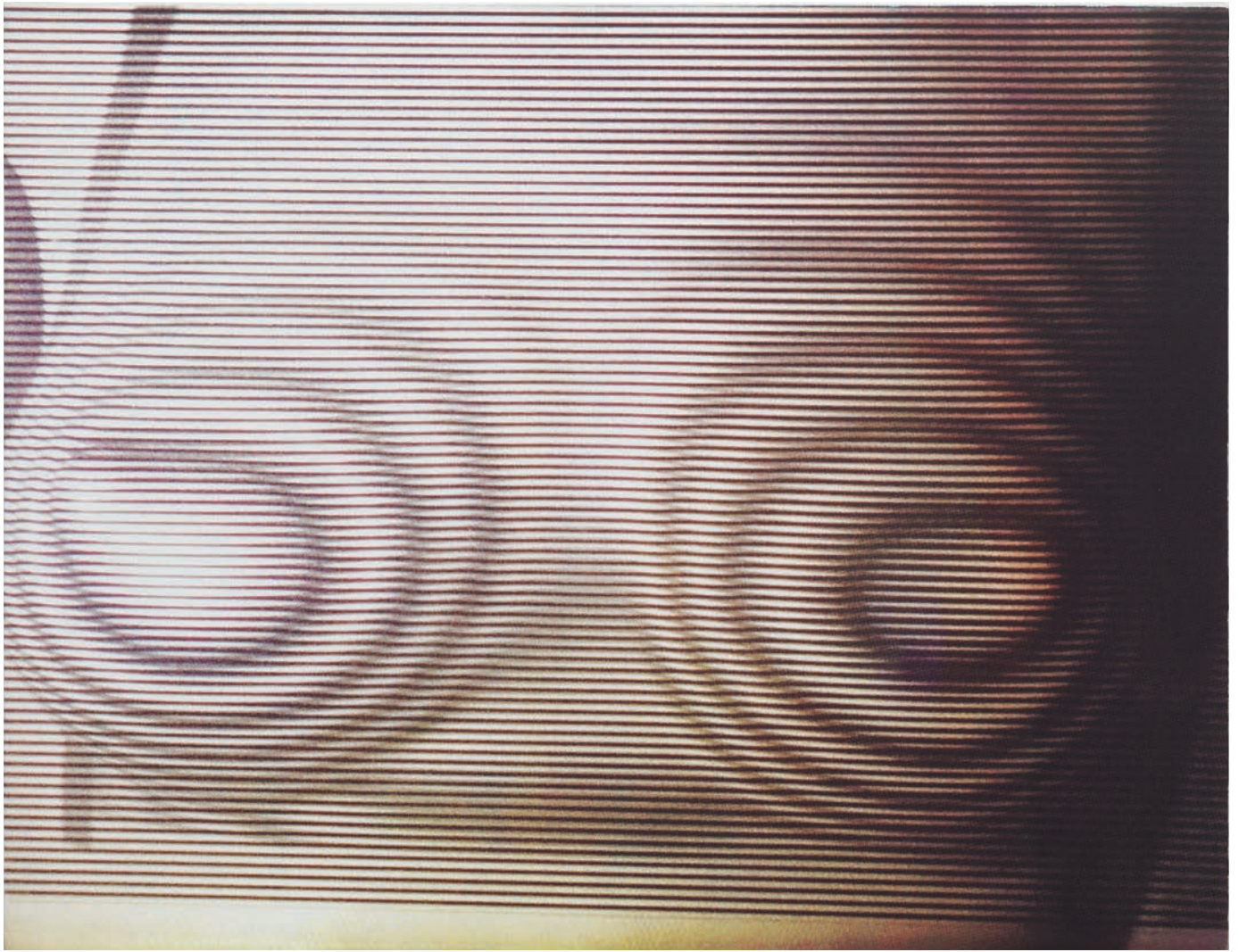




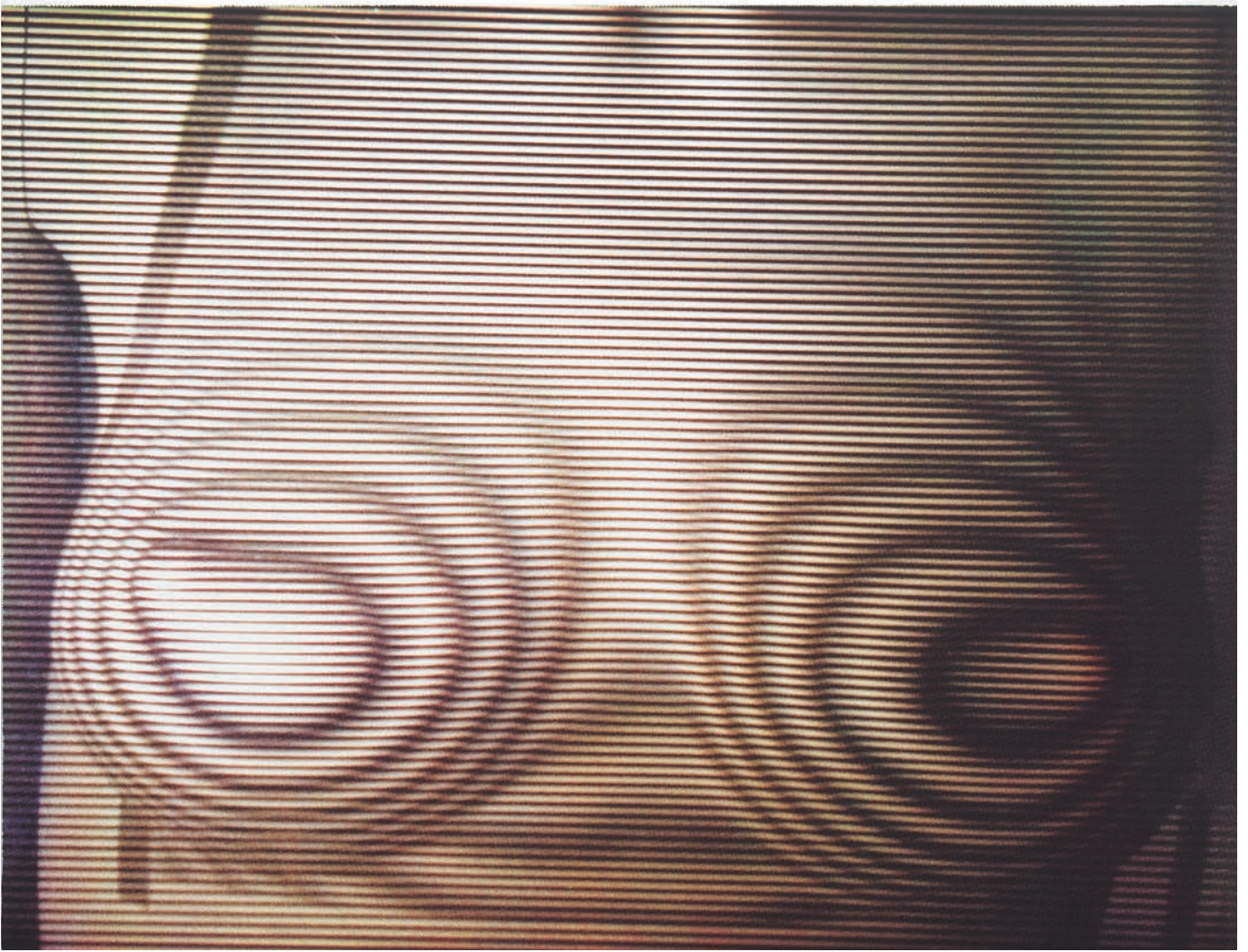
Left:
M1, 2014
acrylic on canvas
142.24 x 91.44 cm / 56 x 36 inches

Above:
M23, 2014
acrylic on canvas
27.94 x 30.48 cm / 11 x 12 inches



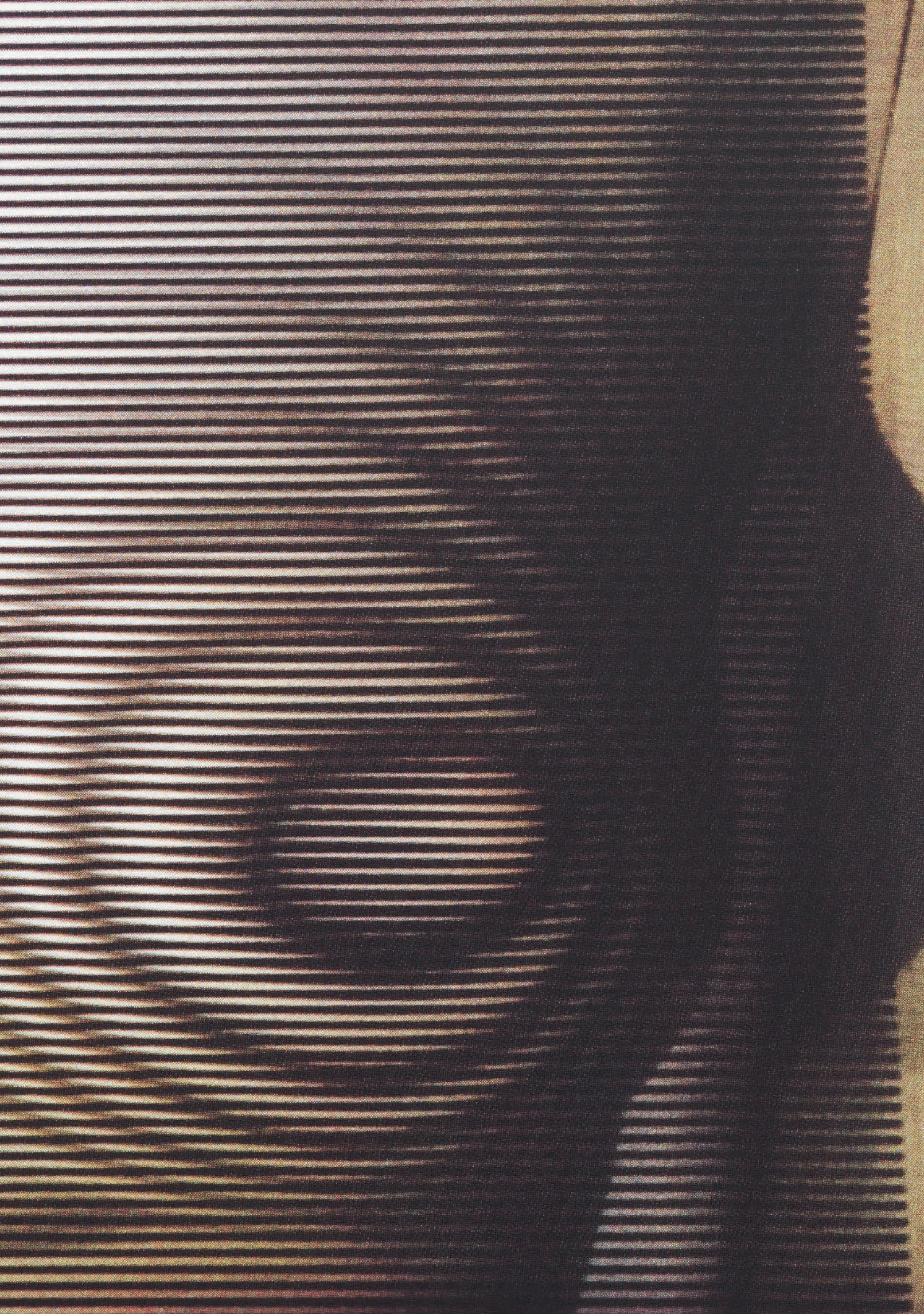


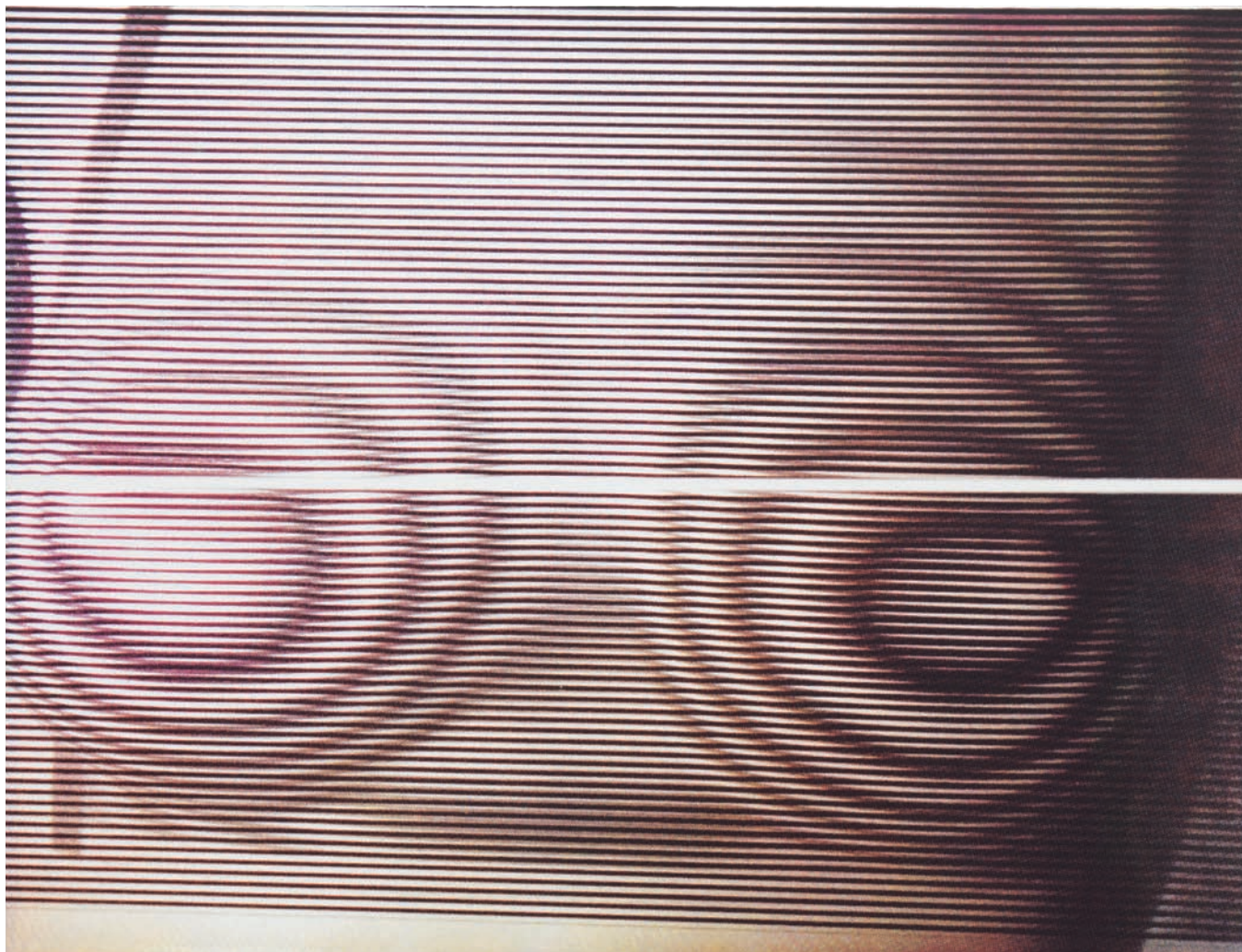
M11, 2014
acrylic on canvas
43.18 x 55.88 cm / 17 x 22 inches



M12, 2014
acrylic on canvas
43.18 x 55.88 cm / 17 x 22 inches

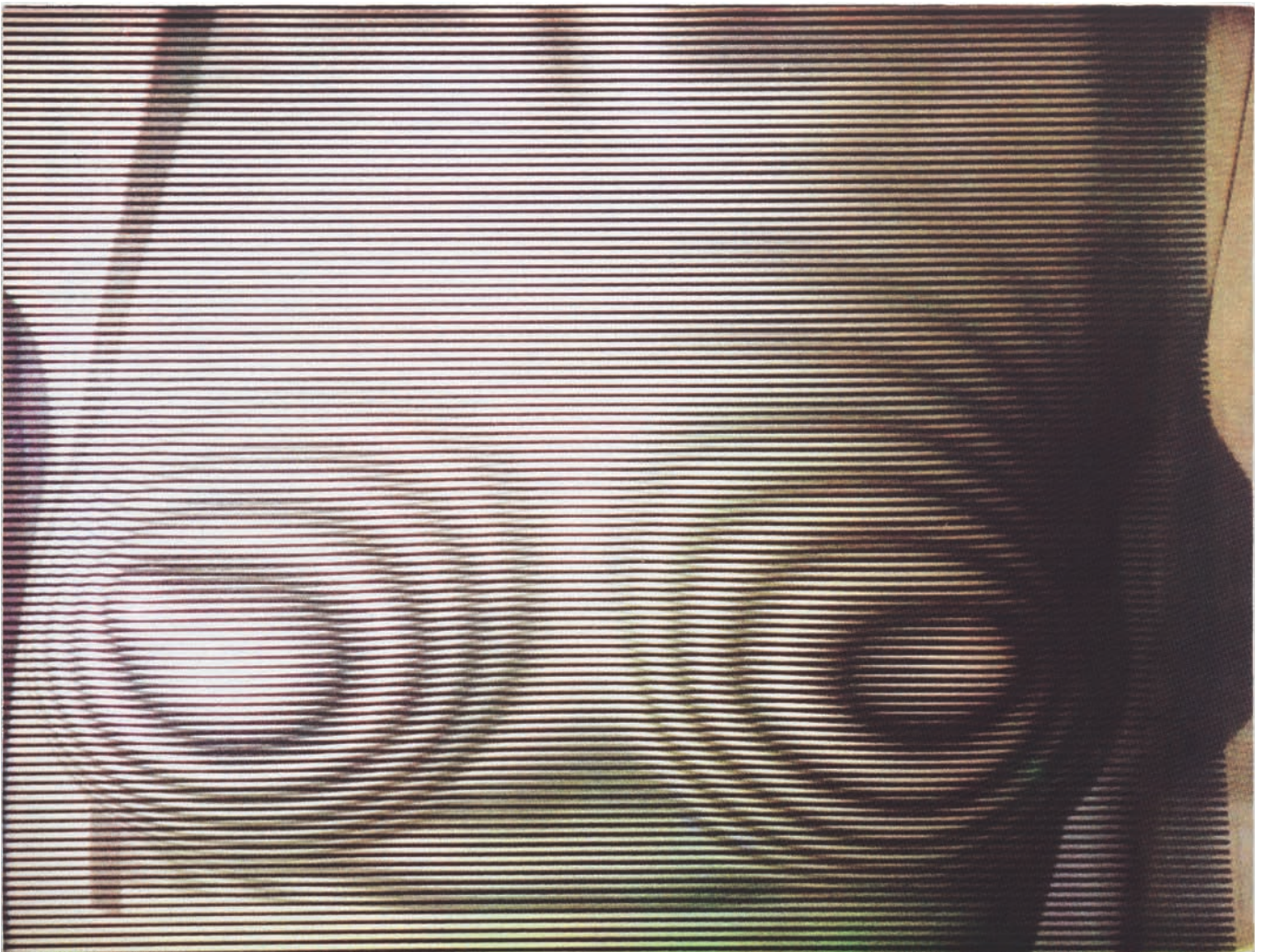




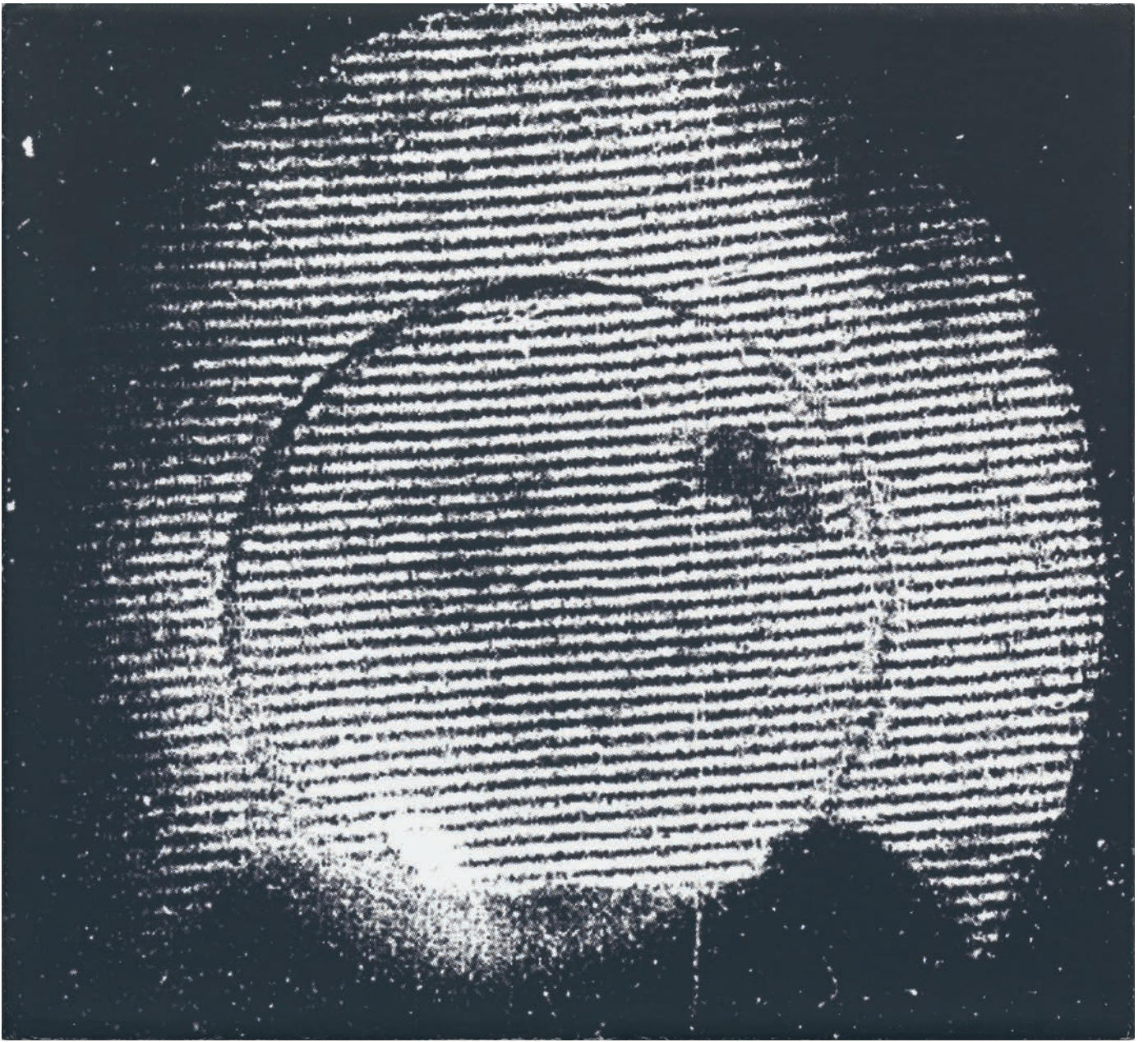


Previous page:
M13-1, 2014 (Detail)
acrylic on canvas
43.18 x 55.88 cm / 17 x 22 inches

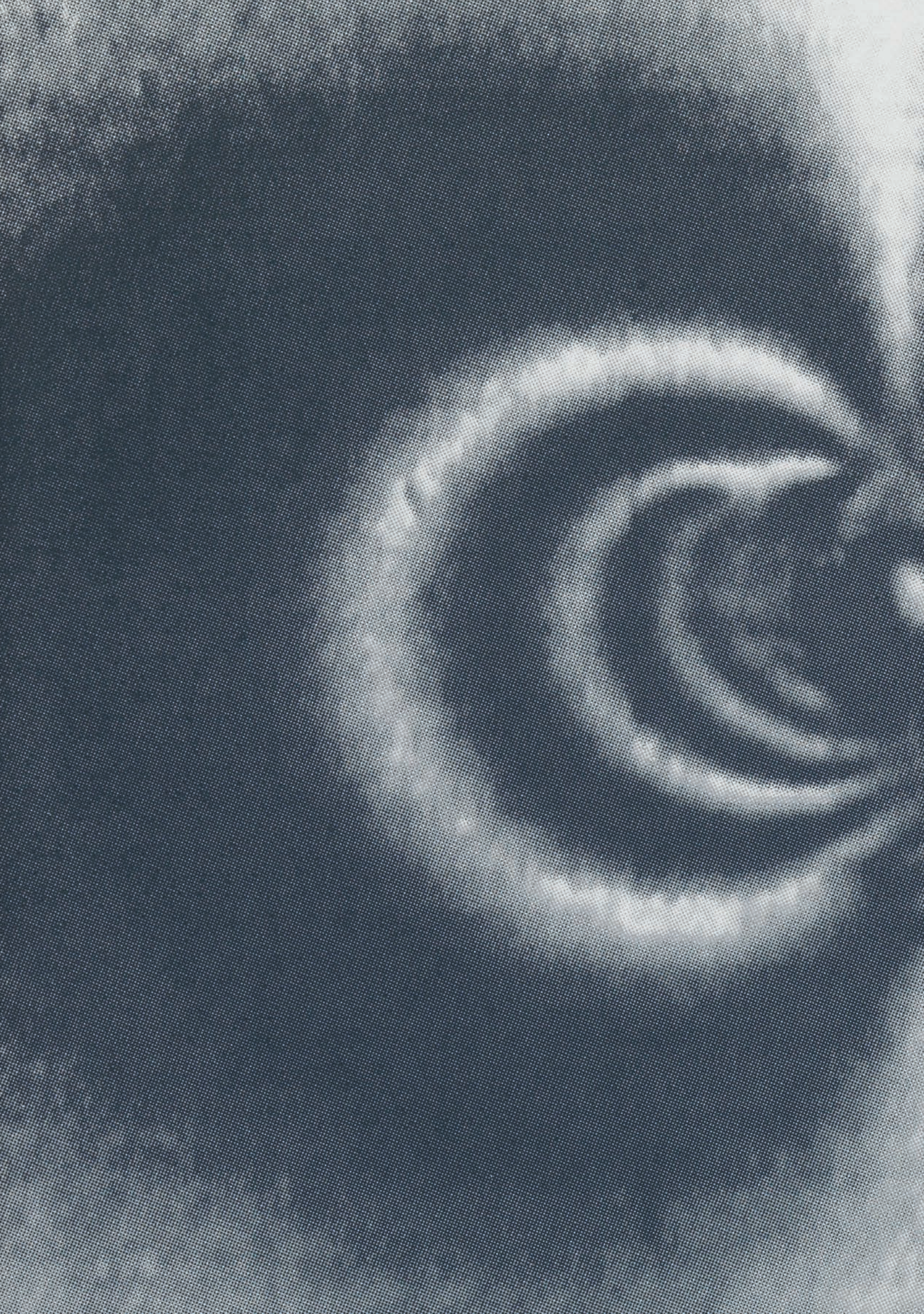
Above:
M15, 2014
acrylic on canvas
43.18 x 55.88 cm / 17 x 22 inches

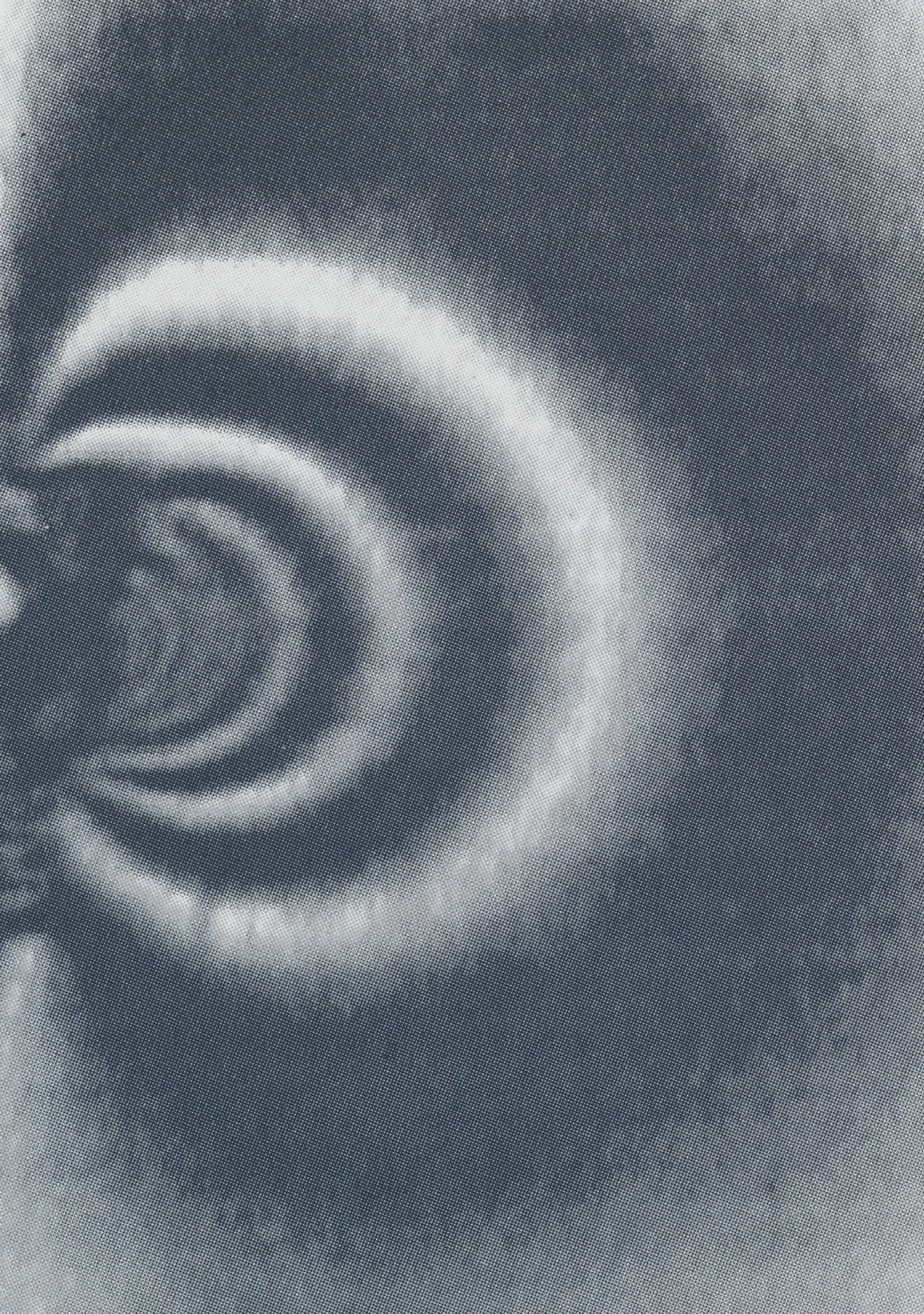


M13-2, 2014
acrylic on canvas
43.18 x 55.88 cm / 17 x 22 inches



M25, 2014
acrylic on canvas
27.94 x 30.48 cm / 11 x 12 inches





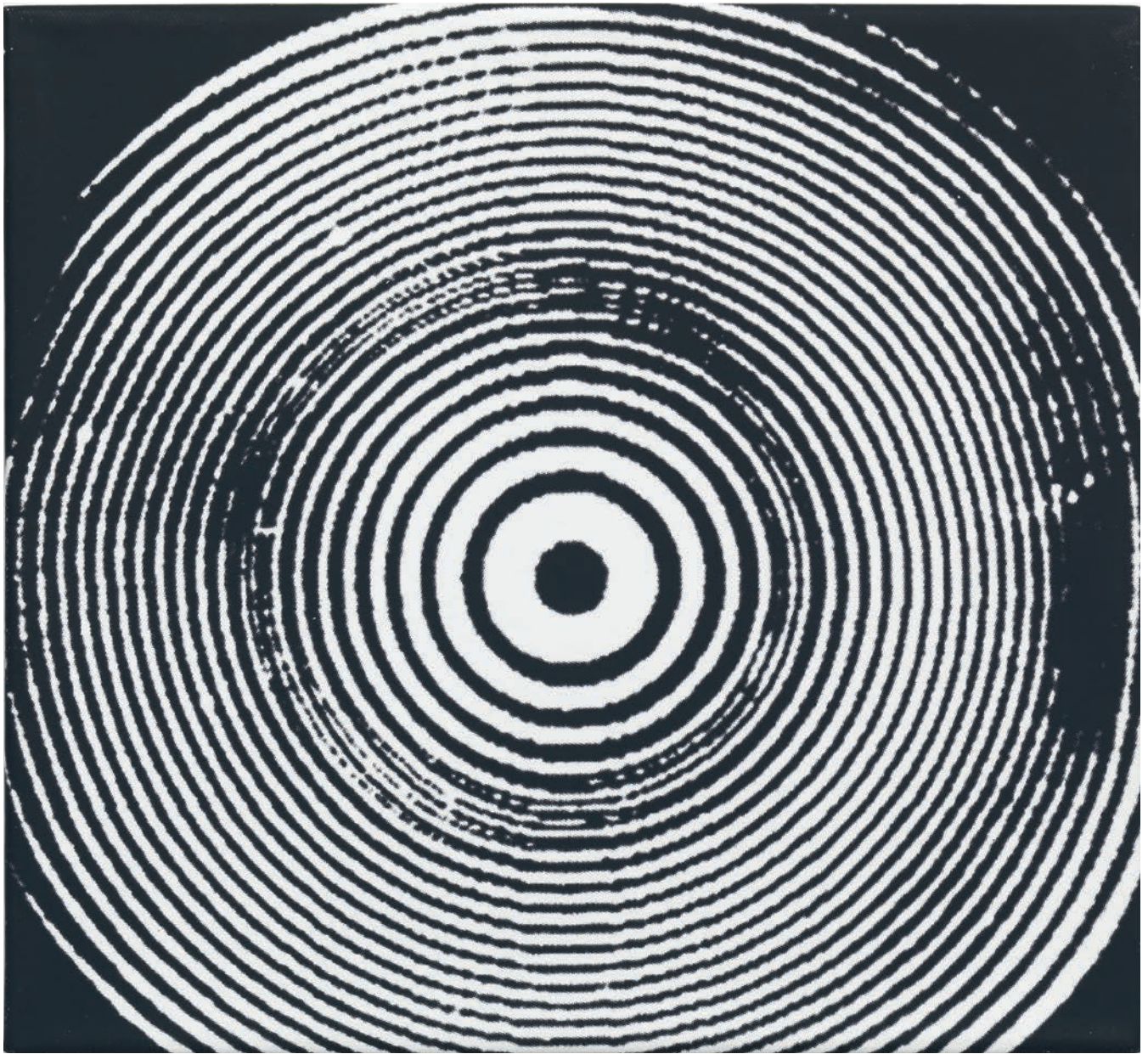


Previous page:
M21, 2014 (Detail)
acrylic on canvas
27.94 x 30.48 cm / 11 x 12 inches

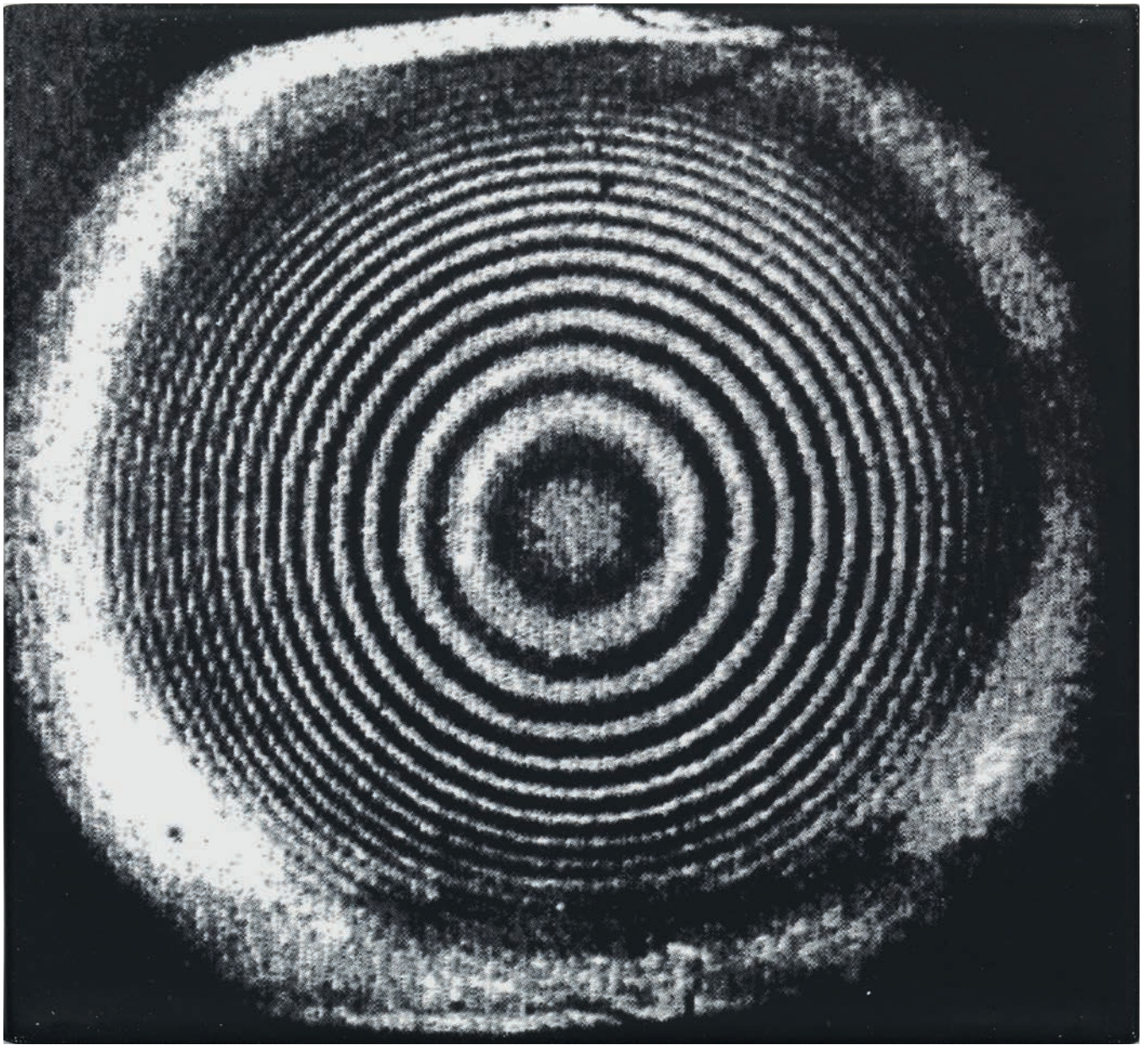
Above:
Das Unheimliche, 2014
Installation view



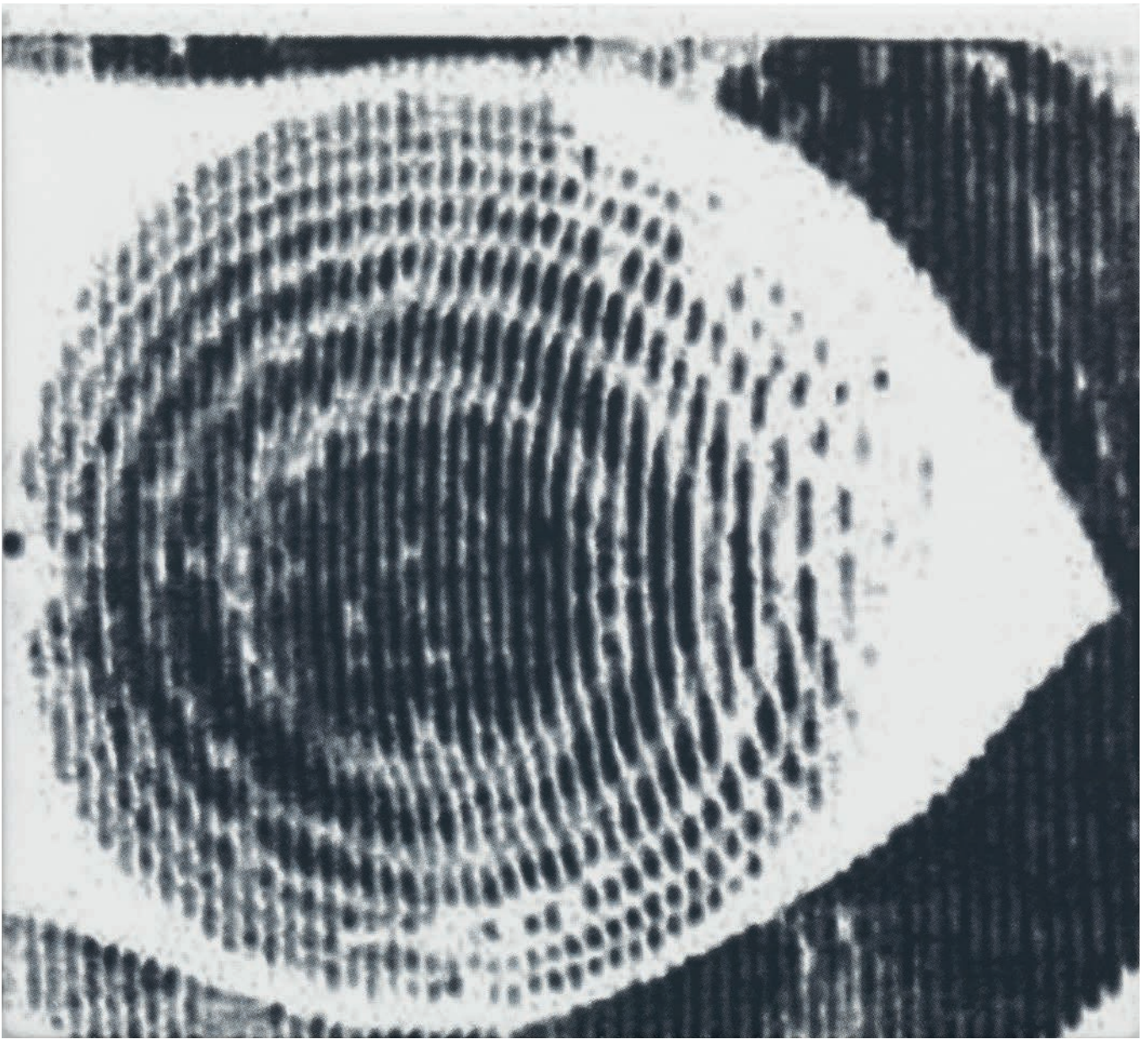
M3, 2014
acrylic on canvas
81.28 x 71.12 cm / 32 x 28 inches



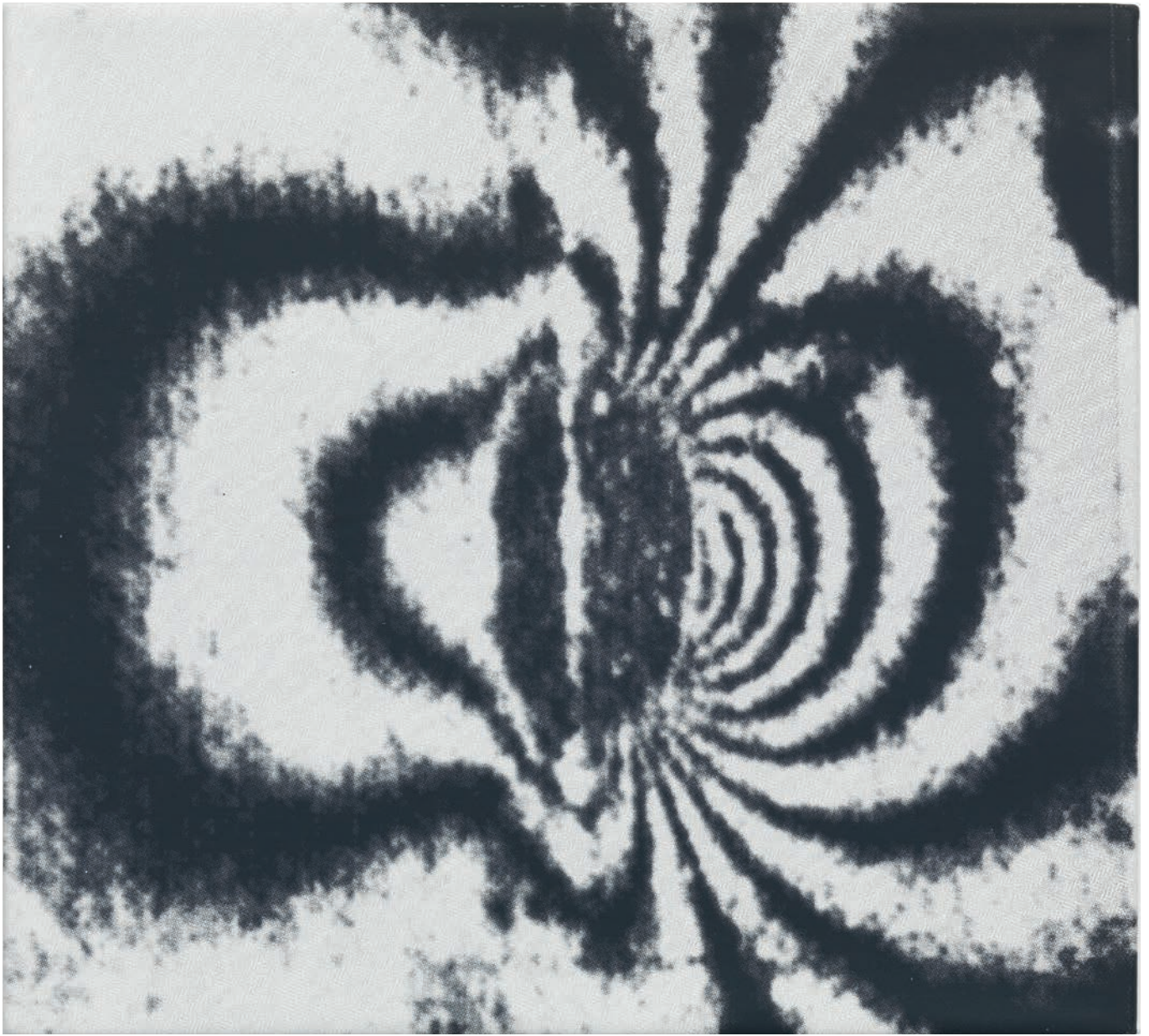
M24, 2014
acrylic on canvas
27.94 x 30.48 cm / 11 x 12 inches



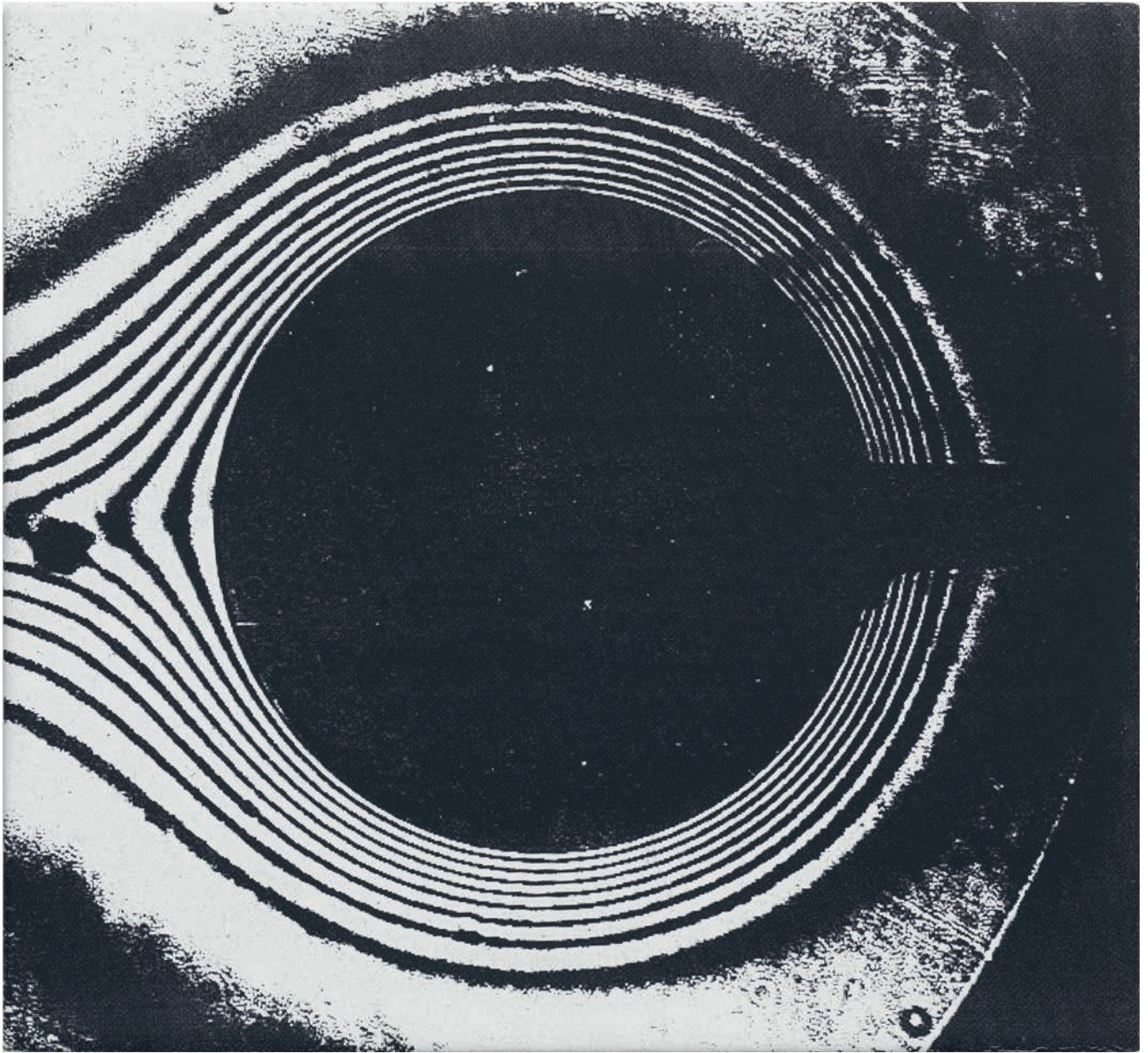
M22, 2014
acrylic on canvas
27.94 x 30.48 cm / 11 x 12 inches



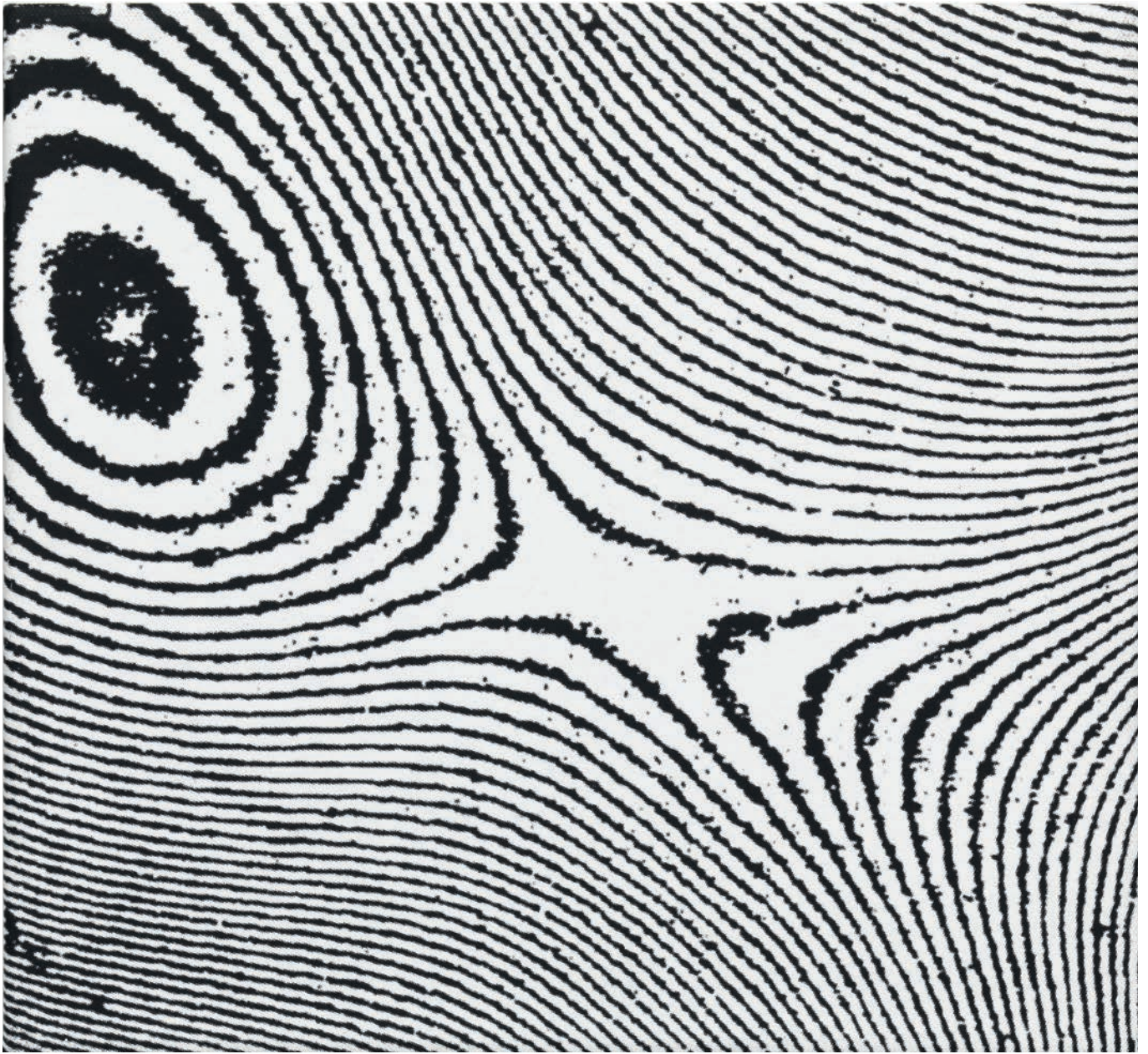
M26, 2014
acrylic on canvas
27.94 x 30.48 cm / 11 x 12 inches



M27, 2014
acrylic on canvas
27.94 x 30.48 cm / 11 x 12 inches



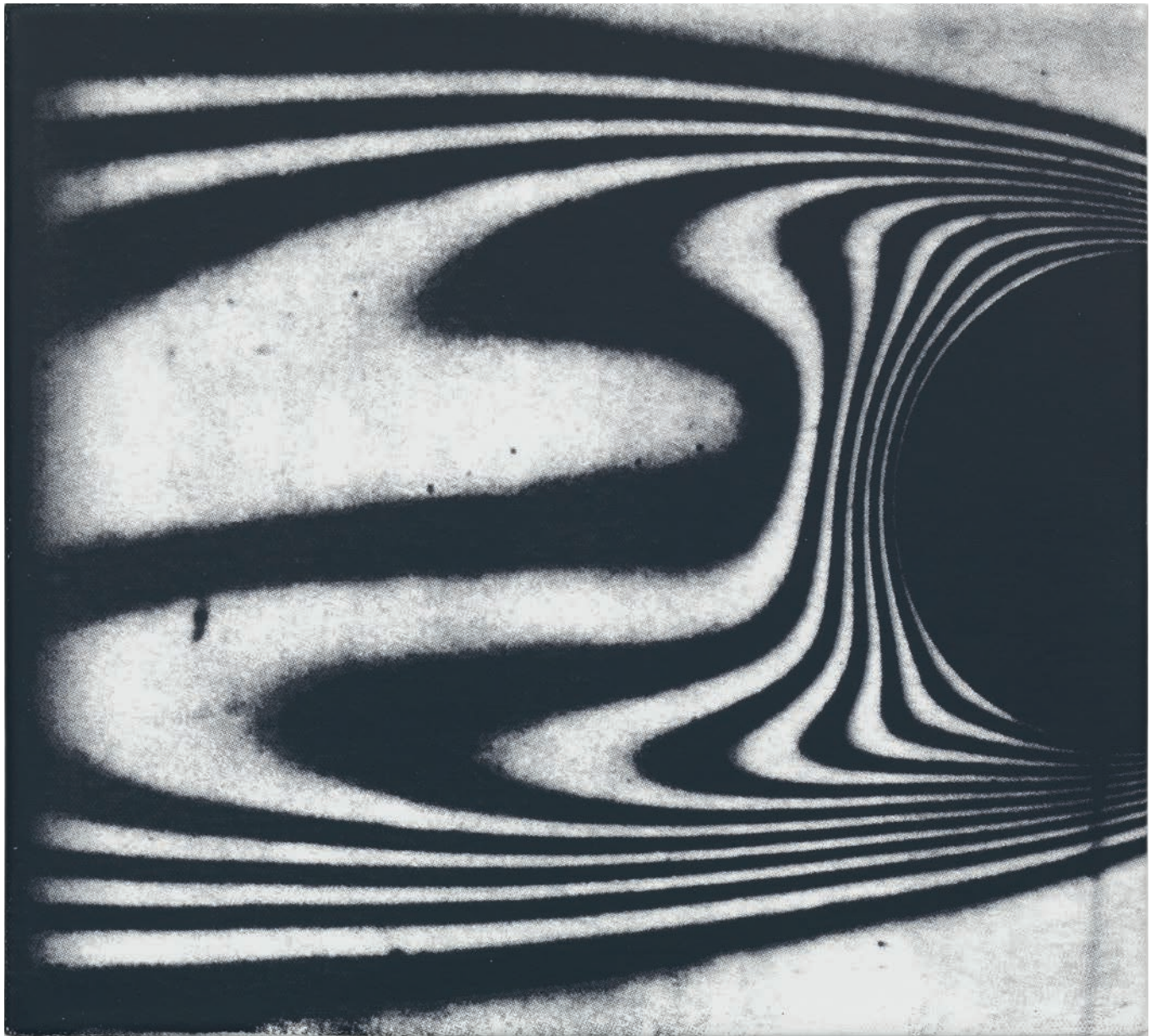
M28, 2014
acrylic on canvas
27.94 x 30.48 cm / 11 x 12 inches



M30, 2014
acrylic on canvas
27.94 x 30.48 cm / 11 x 12 inches

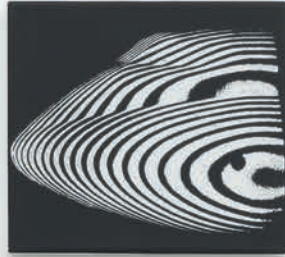


M32, 2014
acrylic on canvas
27.94 x 30.48 cm / 11 x 12 inches



M29, 2014
acrylic on canvas
27.94 x 30.48 cm / 11 x 12 inches

Next page:
M20, 2014
acrylic on canvas
27.94 x 30.48 cm / 11 x 12 inches



ROBERT LAZZARINI

Das Unheimliche

List of works

M2, 2014
acrylic on canvas
134.62 x 83.82 cm / 53 x 33 inches

M1, 2014
acrylic on canvas
142.24 x 91.44 cm / 56 x 36 inches

M23, 2014
acrylic on canvas
27.94 x 30.48 cm / 11 x 12 inches

M11, 2014
acrylic on canvas
43.18 x 55.88 cm / 17 x 22 inches

M12, 2014
acrylic on canvas
43.18 x 55.88 cm / 17 x 22 inches

M13-1, 2014
acrylic on canvas
43.18 x 55.88 cm / 17 x 22 inches

M15, 2014
acrylic on canvas
43.18 x 55.88 cm / 17 x 22 inches

M13-2, 2014
acrylic on canvas
43.18 x 55.88 cm / 17 x 22 inches

M25, 2014
acrylic on canvas
27.94 x 30.48 cm / 11 x 12 inches

M21, 2014
acrylic on canvas
27.94 x 30.48 cm / 11 x 12 inches

M3, 2014
acrylic on canvas
81.28 x 71.12 cm / 38 x 28 inches

M24, 2014
acrylic on canvas
27.94 x 30.48 cm / 11 x 12 inches

M22, 2014
acrylic on canvas
27.94 x 30.48 cm / 11 x 12 inches

M26, 2014
acrylic on canvas
27.94 x 30.48 cm / 11 x 12 inches

M27, 2014
acrylic on canvas
27.94 x 30.48 cm / 11 x 12 inches

M28, 2014
acrylic on canvas
27.94 x 30.48 cm / 11 x 12 inches

M30, 2014
acrylic on canvas
27.94 x 30.48 cm / 11 x 12 inches

M32, 2014
acrylic on canvas
27.94 x 30.48 cm / 11 x 12 inches

M29, 2014
acrylic on canvas
27.94 x 30.48 cm / 11 x 12 inches

M20, 2014
acrylic on canvas
27.94 x 30.48 cm / 11 x 12 inches

This catalog is published on the occasion of the exhibition:

ROBERT LAZZARINI
Das Unheimliche
01 NOVEMBER, 2014 - 10 JANUARY, 2015

**DITTRICH &
SCHLECHTRIEM**

Tucholskystrasse 38 10117 Berlin - Germany

Text: J.B. Allen and D.M. Meadows, *Removal of Unwanted
Patterns from Moiré Contour Maps by Grid Translation
Techniques*, Applied Optics, Vol. 10, No.1, January 1971

Photography: Jens Ziehe
Layout: Owen Reynolds Clements and Vincent Hulme

© 2015, DITTRICH & SCHLECHTRIEM, the artist and authors

Printed in Germany
978-3-945180-03-7

The artist likes to thank:

Owen Reynolds Clements
Luther Davis
Lars Dittrich
Vincent Hulme
Karsten Kretzschmar
André Schleichtriem
Jens Ziehe

